

# B3LYP Calculation of Deuterium Quadrupole Coupling Constants in Molecules

William C. Bailey

*Department of Chemistry and Physics, Kean University, Union, New Jersey 07083*

Received February 4, 1998; in revised form April 1, 1998

The B3LYP/6-31G(df,3p) model for the calculation of deuterium nuclear quadrupole coupling constants (nqcc's) is shown to yield results as accurate as calculations previously performed at the MP4 level of theory. For 25 molecules, ranging from HD and DF to pyridine and fluorobenzene, the rms difference between the B3LYP nqcc's and the experimental nqcc's is 3.2 kHz (2.7%). For benzene, our calculations suggest that the experimental  $\chi_{bb}$  and  $\chi_{cc}$  of S. Jans-Bürli, M. Oldani, and A. Bauder, 1989. *Mol. Phys.*, **68**, 1111–1123) have been incorrectly assigned with respect to inertia axes and should be reversed. For borane carbonyl and nitric acid, it is shown that nqcc calculations using hydrogen bond lengths given by MP2/6-311 + G(d,p) optimizations in combination with the heavy atom experimental structures significantly improve agreement with the experimental nqcc's. © 1998 Academic Press

## INTRODUCTION

The energy of interaction of the electric quadrupole moment of the nucleus of an atom with the molecular electric field gradient (efg) at the site of the nucleus is measured by experimental determination of the nuclear quadrupole coupling constant (nqcc).

Quantum chemistry calculation of the molecular efg permits theoretical prediction of the nqcc, the nqcc being proportional to the efg. For accurate calculation of the efg, the need to include correlation, at least at the level of second-order Møller–Plesset perturbation theory (MP2), in conjunction with a fairly large basis set is generally acknowledged. This requirement, which is demanding of computer resources, places restrictions on the size of the molecule that may be investigated.

Deuterium has been the subject of several quantum chemistry calculations of the efg, including calculations by Gerber and Huber (1) at the level of fourth-order Møller–Plesset perturbation theory (MP4). To extend to fairly large molecules the possibility of calculation at this high level of correlation, these authors employed a large basis set of high quality only on the deuterium atom, with medium-sized bases on neighboring atoms and still smaller bases on atoms further removed.

In a previous paper (2), we have shown that the method developed by Becke (3), which combines density functional theory with Hartree–Fock theory, is a viable alternative to second-order Møller–Plesset perturbation theory (MP2) for calculation of boron nqcc's. This method, known as Becke's three-parameter hybrid method (B3), permits calculations to be performed with computational cost considerably less than perturbation theory.

We report in this paper the results of B3 calculations of the efg (and nqcc) at the site of the deuterium nucleus in a variety

of molecular environments. Our results will be seen to compare favorably with the MP4 calculations of Gerber and Huber. (All MP4 results referred to in this work are those of Gerber and Huber.)

This is followed by a discussion of the results for borane carbonyl, nitric acid, and some other molecules for which experimental coupling constants have been published.

## CALCULATIONS

The components of the nqcc tensor  $\chi_{ij}$  are related to those of the efg tensor  $q_{ij}$  by

$$\chi_{ij} = (eQ/h)q_{ij}, \quad [1]$$

where  $e$  is the proton charge,  $h$  is Planck's constant, and  $Q$  is the electric quadrupole moment of the nucleus.

Experimentally, the coupling constants measurable from the hyperfine spectra are the diagonal elements  $\chi_{aa}$ ,  $\chi_{bb}$ , and  $\chi_{cc}$  of the nqcc tensor, where  $a$ ,  $b$ , and  $c$  are the principal axes of the inertia tensor of the molecule. For direct comparison with the experimental data, the  $q_{ij}$  calculated in this work were transformed to the  $a$ ,  $b$ ,  $c$  system of coordinates.

Following the procedure previously employed (2), the coefficient  $eQ/h$  in Eq. [1] is determined from least-squares, linear regression analysis of the calculated efg's versus the experimental nqcc's. Although not independent, all three diagonal components of the calculated efg tensor are plotted against the corresponding components of the experimental nqcc tensor. This assures, because the tensors are traceless, that the slope of the least-squares line passes through the origin. In this way, the model is calibrated for a selected set of molecules by the best-fit value of  $eQ/h$ , which may then be used for prediction of

nqcc's in other molecules. This empirical procedure is expected to compensate, at least in part, for errors inherent in the model—namely, insufficient correlation and unsaturated bases—and for the effects of zero-point molecular vibrations, for which no correction is made in this work.

All calculations were performed using the Gaussian 94 (4) package of programs. Becke's three-parameter hybrid method was used in conjunction with the correlation functional of Lee *et al.* (5, 6) with double-split valence basis, designated B3LYP/6-31G. Various combinations of polarization functions were incorporated in the basis and investigated for the best linear relationship between the calculated efg's and the experimental nqcc's. These range from one set of *d*-functions on atoms other than hydrogen, and one set of *p*-functions on hydrogen (*d, p*) to three sets of *d*- and one set of *f*-functions on the heavy atoms, and three sets of *p*- and one set of *d*-functions on hydrogen (3*df, 3pd*).

Numerical integrations were performed over a grid consisting of 75 radial shells with 302 angular points per shell (75 × 302) for a total of 22 650 integration points per atom. In several test cases, integrations were performed over a much finer spherical product grid consisting of 96 radial shells around each atom with 32  $\theta$  points and 64  $\varphi$  points per shell, for a total of 196 608 integration points per atom; and over a courser grid, namely the 75 × 302 grid "pruned" to about 7000 integration points per atom (4). No significant differences in the calculated efg were observed among the three grids.

## RESULTS

The molecules and experimental nqcc's (7–15) listed in Table 1 are those selected for calibration of the model. Calculations of the efg's were performed on the equilibrium molecular structures (16–22).

From among the various combinations of polarization functions investigated, the least residual standard deviation and maximum correlation coefficient, 1.55 kHz and 0.99995, respectively, were found for the B3LYP/6-31G(*df, 3p*) model. The least-squares value of  $eQ/h$  for this model is 636.5 (13) kHz/a.u.

For the MP4 model of Gerber and Huber, although the set of molecules used for calibration differs from that used in this work, their value of  $eQ/h$  (calculated from the data reported by these authors) is 635.8 kHz/a.u., which lies within one standard error in the above value.

The nqcc's calculated with the B3LYP/6-31G(*df, 3p*) model for the nine molecules used for calibration are shown in Table 1, along with the MP4 results and the experimental values. With one notable exception, the B3LYP and MP4 values are comparable (although, in some cases, different molecular structures may have been used for the calculations), and both models compare favorably with the experimental values. The exception is CF<sub>3</sub>D, for which the B3LYP nqcc of 167.4 kHz approximates the experimental value of 170.8 kHz, while the

TABLE 1  
Nuclear Quadrupole Coupling Constants (kHz)

Molecule	ij	B3LYP	MP4 <sup>a</sup>	Expt.	References	
					nqcc/struct.	
DF	aa	354.7	354.8	354.238 (78)	7	16
DCl	aa	186.5	186.7	188.8 (30)	8	16
DBr	aa	145.7		146.9 (14)	9	16
CH <sub>3</sub> D	aa	193.1	189.6	191.48 (77)	10	17
D <sub>2</sub> S	aa	52.68		51.84 (17)	11	18
	bb	36.56		36.54 (13)		
	cc	-89.24	-89.4	-88.38 (11)		
	ab	±109.1		109.24 (31)		
DCN	aa	204.5	201.9	200.6 (5)	12	19
D <sub>2</sub> CO	aa	-13.84		-12.53 (10)	13	20
	bb	96.90		97.23 (10)		
	cc	-83.06	-85.2	-84.70 (10)		
	ab	±113.5				
CF <sub>3</sub> D	aa	167.4	152.1	170.8 (20)	14	21
HCOOD	aa	-118.9	-117.2	-119.3 (20)	15	22
	bb	267.1	269.4	267.5 (30)		
	cc	-148.2	-153.1	-148.2 (20)		
	ab	-25.5				

<sup>a</sup> Ref. (1).

MP4 model predicts a nqcc of 152.1 kHz. In this case, it appears that a less accurate molecular structure was used for the MP4 calculation.

Additional molecules for which experimental nqcc's (23–34) and molecular structures (35–45) are available are listed in Table 2. The results of B3LYP calculations of the nqcc's for these molecules, along with the MP4 results, are also given in this table. Where MP4 results are available, it is seen that the B3LYP model yields comparable nqcc's. For CD<sub>3</sub>CCH and CD<sub>3</sub>CN, where the B3LYP and MP4 results are somewhat different, different structures were used for the calculations. The more recent structures (39, 40) used in this work produce better agreement with the experimental nqcc's.

In Table 3, the experimental (46) and calculated nqcc's are compared for benzene and fluorobenzene. The structures on which the calculations were made are those given by Olandi and Bauder (47) for benzene, and Doraiswamy and Sharma (48) for fluorobenzene.

It would appear, in the case of benzene, that the experimental  $\chi_{bb}$  and  $\chi_{cc}$  have been incorrectly assigned. This conclusion is suggested by our calculations, and supported by the experimental results for fluorobenzene-4-d<sub>1</sub>. One would expect the nqcc's for benzene-d<sub>1</sub> and fluorobenzene-4-d<sub>1</sub> to be similar.

Figure 1 shows, for the convenience of visual comparison, a plot of the B3LYP efg's versus the experimental nqcc's. The solid circles in the plot are the molecules of Table 1 used for calibration of the model, and the open circles are those of Tables 2 and 3. For all 25 molecules in Tables 1–3, the root

TABLE 2  
Nuclear Quadrupole Coupling Constants (kHz)

Molecule	ij	B3LYP	MP4 <sup>a</sup>	Expt.	References	
					nqcc/struct.	
HD	aa	224.0		224.54(6)	23	35
D <sub>2</sub>	aa	223.9		225.044(24)	24	35
D <sub>2</sub> O	aa	148.9		153.92(11)	25	36
	bb	24.9		22.12(11)		
	cc	-173.8	-172.1	-175.037(11)		
	ab	±209.6				
ND <sub>3</sub>	aa	201.3	202.1	207	26	37
	bb	-107.8	-108.4	-111		
	cc	-93.4	-94.6	-96		
	ab	-133.7				
BD <sub>3</sub> CO	aa	-44.70		-48.5(23)	27	38
CD <sub>3</sub> CCH	aa	-55.17	-52.1	-55.0(5)	28	39
CD <sub>3</sub> CN	aa	-56.05	-51.7	-55.1(4)	29	40
CD <sub>3</sub> Cl	aa	-59.26	-60.0	-59.3(16)	30	41
DNCO	aa	53.1		57.6(54)	31	42
	bb	92.4		84.9(29)		
	cc	-145.5	-145.0	-142.5(29)		
	ab	206.6				
DNCS	aa	100.0		94.8(26)	32	43
	bb	41.9		40.5(14)		
	cc	-141.8		-135.3(14)		
	ab	-207.8				
DNSO	aa	-110.1		-114.9(31)	33	44
	bb	219.4		225.4 <sup>b</sup>		
	cc	-109.3		-110.5 <sup>b</sup>		
	ab	-12.7				
Pyridine	aa	196.0		196(4)	34	45
	bb	-94.1		-90(8)		
	cc	-101.9		-106(8)		

<sup>a</sup> Ref. (1).

<sup>b</sup> Derived from  $\chi_{aa}$ , and  $\chi_{bb} - \chi_{cc} = 336.0(31)$  kHz. Ref. (33).

mean square (rms) difference between the calculated and experimental nqcc's is 3.2 kHz (assuming that the experimental  $\chi_{bb}$  and  $\chi_{cc}$  for benzene are reversed), which is 2.7% of the average absolute experimental nqcc. This result is essentially the same as that of Gerber and Huber, who claim for their MP4 calculations an accuracy better than 3% in general, albeit for somewhat different experimental data.

Agreement in the value of  $eQ/h$  between the B3LYP and MP4 models, together with agreement in the rms deviation, implies little difference in the values of the calculated efg's.

## DISCUSSION

For borane carbonyl, both boron (BH<sub>3</sub>CO) and deuterium (BD<sub>3</sub>CO) nqcc's have been measured. These results are given

in Table 4 along with the calculated values using the experimental ( $r_s$ ) structure of Venkatachar *et al.* (38). Calculation of the boron nqcc was made using the B3LYP/6-31G(*df,p*) model with  $eQ/h = 9.673(40)$  MHz/a.u. (2). The calculated and experimental nqcc's are as follows: for boron, 1.604 and 1.6619 MHz, respectively; and for deuterium, -44.7 and -48.5 kHz.

To investigate the dependence on structure, the geometry of the molecule was optimized using the MP2/6-311 + G(*d,p*) model (triple-split valence basis with diffuse functions on the heavy atoms), and the nqcc's were recalculated. The optimized and experimental structures are compared in Table 5; the recalculated nqcc's are given in Table 4. There is, as shown in Table 4, improvement in the deuterium nqcc. For boron, how-

TABLE 3  
Benzene and Fluorobenzene Nuclear Quadrupole  
Coupling Constants (kHz)

Molecule	B3LYP	Expt. <sup>a</sup>
Benzene-d <sub>1</sub>	aa 192.2	186.1 (18)
	bb -90.7	-97.2 (23)
	cc -101.5	-88.9 (23)
Fluorobenzene-4-d <sub>1</sub>	aa 194.6	187.7 (15)
	bb -91.2	-89.0 (30)
	cc -103.4	-98.7 (25)
-3-d <sub>1</sub>	aa -12.8	-9.6 (33)
	bb 113.2	112.6 (32)
	cc -100.4	-103.0 (26)
	ab ±125.2	
-2-d <sub>1</sub>	aa -9.7	-18.0 (26)
	bb 111.8	115.7 (27)
	cc -102.1	-97.7 (22)
	ab ±127.9	

<sup>a</sup> Ref. (46).

ever, the calculated nqcc is now further from agreement with the experimental value. This suggests that the BH bond length is more accurately approximated by the *ab initio* optimization, but that the heavy atom bond lengths are more accurately given by the  $r_s$  structure. The HBH angle is essentially the same for both structures, differing by only 0.2°.

Therefore, a second recalculation was made using the heavy atom  $r_s$  structure with the BH<sub>3</sub> geometry given by the MP2 optimization. These results, under the heading  $r_s$ /MP2 in Table 4, agree very well with the experimental nqcc's for both boron and deuterium. For boron, the calculated nqcc is now 1.655 MHz (expt., 1.6619 MHz); for deuterium, -48.6 kHz (expt., -48.5 kHz).

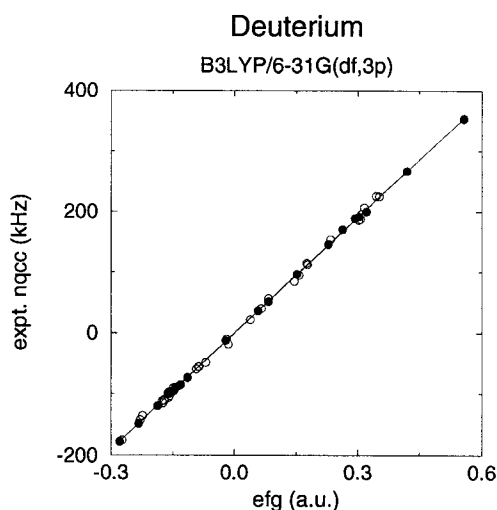


FIG. 1. B3LYP/6-31G(df,3p) efg's versus experimental nqcc's. The solid circles represent the molecules of Table 1 used for calibration of the theoretical model. The open circles are the molecules of Tables 2, 3.

TABLE 4  
Borane Carbonyl D and <sup>11</sup>B Quadrupole  
Coupling Constants

		B3LYP			Expt.
		$r_s^a$	MP2 <sup>b</sup>	$r_s$ /MP2 <sup>c</sup>	
D	aa	-44.7	-48.2	-48.6	-48.5 (23) <sup>d</sup> kHz
<sup>11</sup> B	aa	1.604	1.844	1.655	1.6619 (23) <sup>e</sup> MHz

<sup>a</sup> Ref. (38).

<sup>b</sup> MP2/6-311 + G(d,p) optimization. See Table 5.

<sup>c</sup> Heavy atom  $r_s$  structure with MP2 BH<sub>3</sub> structure.

<sup>d</sup> Ref. (27).

<sup>e</sup> A. Murray and S. Kukolich, J. Chem. Phys. 77, 4312-4317 (1982).

This result, which may be fortuitous, does suggest that the experimental BH bond length is probably too long. The *ab initio* value of the BH bond length is 1.205 Å compared with the  $r_s$  value of 1.222 Å.

The experimental (49) and calculated nqcc's for nitric acid, D<sup>15</sup>NO<sub>3</sub>, are summarized in Table 6. Whereas the B3LYP and MP4 (49) results are similar, neither approximates the experimental nqcc's. For  $\chi_{cc}$ , for example, the difference between the B3LYP and experimental values is 14.1 kHz (9.4%). For all three diagonal coupling constants, the rms difference is 12.3 kHz.

These calculations, both B3LYP and MP4, were performed on the experimental structure given by Ghosh *et al.* (50), hereafter referred to as GBB. Encouraged by the results for borane carbonyl, the molecular structure was optimized using the MP2/6-311 + G(d,p) model. Taking the heavy atom structure of GBB with the *ab initio* NOD angle and OD bond length, the nqcc's were recalculated. These are shown in Table 6.

TABLE 5  
Molecular Structure of Borane Carbonyl and  
Experimental  $r_s$  and *Ab Initio* MP2/6-311 +  
G(d,p)

	$r_s^a$	MP2
BC	1.534 ± 0.01	1.553
CO	1.135 ± 0.01	1.138
BH	1.222 ± 0.001	1.205
∠HBC	103.8 ± 0.06	104.0
∠HBH	114.5 ± 0.15	114.3

Note. Bond lengths in Å and bond angles in degrees.

<sup>a</sup> Ref. (38).

TABLE 6  
D<sup>15</sup>NO<sub>3</sub> Nuclear Quadrupole Coupling  
Constants (kHz)

	GBB <sup>a</sup>		GBB/MP2 <sup>b</sup>	
	B3LYP	MP4 <sup>c</sup>	B3LYP	Expt. <sup>c</sup>
aa	29.4	30.3	31.3	31.1 (24)
bb	134.3	135.3	122.8	118.5 (29)
cc	-163.7	-166.5	-154.2	-149.6 (29)
ab	187.0	184.2	176.0	

<sup>a</sup> Ghosh *et al.* (50).

<sup>b</sup> Ghosh *et al.* heavy atom structure with *ab initio* MP2/6-311 + G(*d,p*) NOD angle and OD bond length.

<sup>c</sup> Ref. (49).

Agreement with the experimental nqcc's is notably improved, the difference between the calculated and experimental values of  $\chi_{cc}$  reduced to 4.6 kHz (3.1%). For all three diagonal coupling constants, the rms difference is now 3.6 kHz, which is in line with the overall result of this work.

The MP2 value of the OD bond length is 0.971 Å, and the GBB value is 0.962 Å; the MP2 value of the NOD angle is 102.8°, and the GBB value is 102.3°.

In the case of deuterioacetylene, there have been a number of measurements of the deuterium nqcc in different excited states. Approximations to the ground state value have been reported by DeLeon and Muentner (51), and Marshall and Klemperer (52). The former measured 208.5(9) kHz, the latter 221(2) kHz. In deuteriodiacetylene, Böttcher *et al.* (53) report a nqcc of 217(6) kHz. The MP4 and B3LYP values of the nqcc are 211.8 and 214.1 kHz, respectively. The B3LYP calculation was performed on the equilibrium structure of acetylene given by Baldacci *et al.* (54).

Cogley *et al.* (28) report for CH<sub>3</sub>CCD a coupling constant of 228(2), while an earlier paper by Weiss and Flygare (55) reports a value of 208(10) kHz. The MP4 value is 214.9 kHz, and the B3LYP value is 217.9 kHz. For the latter calculation, the near equilibrium structure of Le Guennec *et al.* (39) was used.

Three measurements of the nqcc for deuterated cyanoacetylene are found in the literature: 198.2(46) (56), 228.8(55) (57), and 203.5(15) kHz (58). The MP4 and B3LYP values are, respectively, 213.0 and 211.5 kHz. The equilibrium structure of Botschwina *et al.* (59) was used for the B3LYP calculation.

For HCP, an equilibrium structure has been reported by Strey and Mills (60). The experimental value of the nqcc in DCP is 233(40) kHz (61). The B3LYP nqcc is 207 kHz, which lies within the large uncertainty in the experimental value.

Verma *et al.* (62) have determined a substitution structure for diazirine-*d*<sub>2</sub>, and measured  $\chi_{aa} = -33(20)$  and  $\chi_{bb} = -105(10)$  kHz. The B3LYP values of these constants are,

respectively, -16.5 and 105.8 kHz, both of which lie within the large uncertainties in the experimental values.

Finally, for LiD, using the equilibrium structure of Pearson and Gordy (63), the B3LYP nqcc is 44 kHz. The experimental value is 33(1) kHz (64).

## CONCLUSION

In conclusion, nqcc's calculated from B3LYP/6-31G(*df,3p*) efg's agree with the experimental nqcc's (for the 25 molecules in Tables 1–3) with a rms difference of 3.2 kHz, which is 2.7% of the average absolute experimental nqcc. This result is comparable to that reported by Gerber and Huber for their MP4 calculations.

For benzene, our calculations suggest an incorrect assignment of the experimental  $\chi_{bb}$  and  $\chi_{cc}$  with respect to the inertia axes, the values should be reversed.

It is shown for borane carbonyl and nitric acid that calculations done on structures that combine hydrogen bond lengths given by MP2/6-311 + G(*d,p*) geometries with the experimental heavy atom structures significantly improve agreement with the experimental nqcc's.

For the acetylenes there are large differences between the calculated and experimental nqcc's, but there are large differences also between experimental values. For LiD, the difference between the calculated and experimental nqcc is large.

## REFERENCES

1. S. Gerber and H. Huber, *J. Mol. Spectrosc.* **134**, 168–175 (1989).
2. W. Bailey, *J. Mol. Spectrosc.* **185**, 403–407 (1997).
3. A. Becke, *J. Chem. Phys.* **98**, 5648–5652 (1993).
4. M. J. Frisch, G. W. Trucks, H. B. Schlegel, P. M. W. Gill, B. G. Johnson, M. A. Robb, J. R. Cheeseman, T. Keith, G. A. Petersson, J. A. Montgomery, K. Raghavachari, M. A. Al-Laham, V. G. Zakrzewski, J. V. Ortiz, J. B. Foresman, J. Cioslowski, B. B. Stefanov, A. Nanayakkara, M. Challacombe, C. Y. Peng, P. Y. Ayala, W. Chen, M. W. Wong, J. L. Andres, S. Replogle, R. Gomperts, R. L. Martin, D. J. Fox, J. S. Binkley, D. J. Defrees, J. Baker, J. P. Stewart, M. Head-Gorden, C. Gonzalez, and J. A. Pople, "Gaussian 94, Revision B1," Gaussian, Inc., Pittsburgh, PA, 1995.
5. C. Lee, W. Yang, and R. G. Parr, *Phys. Rev. B* **37**, 785–789 (1988).
6. B. Miehlich, A. Savin, H. Stoll, and H. Preuss, *Chem. Phys. Lett.* **157**, 200–206 (1989).
7. J. S. Muentner and W. Klemperer, *J. Chem. Phys.* **52**, 6033–6037 (1970).
8. E. W. Kaiser, *J. Chem. Phys.* **53**, 1686–1703 (1970).
9. B. P. Van Eijck, *J. Mol. Spectrosc.* **53**, 246–249 (1974).
10. S. C. Wofsy, J. S. Muentner, and W. Klemperer, *J. Chem. Phys.* **53**, 4005–4014 (1970).
11. R. Viswanathan and T. R. Dyke, *J. Mol. Spectrosc.* **103**, 231–239 (1984).
12. G. Cazzoli and L. Dore, *J. Mol. Spectrosc.* **143**, 231–236 (1990).
13. K. D. Tucker and G. R. Tomasevich, *J. Mol. Spectrosc.* **48**, 475–478 (1973).
14. S. G. Kukolich, A. C. Nelson, and D. J. Ruben, *J. Mol. Spectrosc.* **40**, 33–39 (1971).
15. D. J. Ruben and S. G. Kukolich, *J. Chem. Phys.* **60**, 100–102 (1974).
16. F. C. De Lucia, P. Helminger, and W. Gordy, *Phys. Rev. A* **3**, 1849–1857 (1971).

17. D. L. Gray and A. G. Robiette, *Mol. Phys.* **37**, 1901–1920 (1979).
18. T. H. Edwards, N. K. Moncur, and L. E. Snyder, *J. Chem. Phys.* **46**, 2139–2142 (1967).
19. S. Carter, I. M. Mills, and N. C. Handy, *J. Chem. Phys.* **97**, 1606–1607 (1992).
20. S. Carter and N. C. Handy, *J. Mol. Spectrosc.* **179**, 65–72 (1996).
21. Y. Kawashima and A. P. Cox, *J. Mol. Spectrosc.* **72**, 423–429 (1978).
22. R. W. Davis, A. G. Robiette, M. C. L. Gerry, E. Bjarnov, and G. Winnewisser, *J. Mol. Spectrosc.* **81**, 93–109 (1980).
23. W. E. Quinn, J. M. Baker, J. T. LaTourrette, and N. F. Ramsey, *Phys. Rev.* **112**, 1929–1940 (1958).
24. R. F. Code and N. F. Ramsey, *Phys. Rev. A* **4**, 1945–1959 (1971).
25. R. Bhattacharjee, J. S. Muentner, and M. D. Marshall, *J. Mol. Spectrosc.* **145**, 302–307 (1991).
26. J. Cederberg, *J. Mol. Spectrosc.* **77**, 102–108 (1979).
27. A. M. Murray and S. G. Kukolich, *J. Chem. Phys.* **77**, 4312–4317 (1982).
28. C. D. Cogley, L. M. Tack, and S. G. Kukolich, *J. Chem. Phys.* **76**, 5669–5671 (1982).
29. A. M. Murray and S. G. Kukolich, *J. Chem. Phys.* **78**, 3557–3559 (1983).
30. S. G. Kukolich, *J. Chem. Phys.* **55**, 4488–4493 (1971).
31. N. Heineking, M. C. L. Gerry, and H. Dreizler, *Z. Naturforsch.* **44a**, 577–579 (1989).
32. N. Heineking and H. Dreizler, *Z. Naturforsch.* **47a**, 511–514 (1991).
33. N. Heineking and M. C. L. Gerry, *J. Mol. Spectrosc.* **158**, 62–68 (1993).
34. N. Heineking, H. Dreizler, and R. Schwarz, *Z. Naturforsch.* **41a**, 1210–1213 (1986).
35. B. P. Stoicheff, *Can. J. Phys.* **35**, 730–741 (1957).
36. W. S. Benedict, N. Gailar, and E. K. Plyler, *J. Chem. Phys.* **24**, 1139–1156 (1956).
37. J. D. Swalen and J. A. Ibers, *J. Chem. Phys.* **36**, 1914–1918 (1962).
38. H. C. Venkatachar, R. C. Taylor, and R. L. Kuczkowski, *J. Mol. Struct.* **38**, 17–23 (1977).
39. M. Le Guennec, J. Demaison, G. Wlodarczak, and C. J. Marsden, *J. Mol. Spectrosc.* **160**, 471–490 (1993).
40. M. Le Guennec, G. Wlodarczak, J. Burie, and J. Demaison, *J. Mol. Spectrosc.* **154**, 305–323 (1992).
41. M. Imachi, T. Tanaka, and E. Hirota, *J. Mol. Spectrosc.* **63**, 265–280 (1976).
42. K. Yamada, *J. Mol. Spectrosc.* **79**, 323–344 (1980).
43. K. Yamada, M. Winnewisser, G. Winnewisser, L. B. Szalanski, and M. C. L. Gerry, *J. Mol. Spectrosc.* **79**, 295–313 (1980).
44. W. H. Kirchhoff, *J. Am. Chem. Soc.* **91**, 2437–2442 (1969).
45. B. Bak, L. Hansen-Nygaard, and J. Rastrup-Andersen, *J. Mol. Spectrosc.* **2**, 361–368 (1958).
46. S. Jans-Bürli, M. Oldani, and A. Bauder, *Mol. Phys.* **68**, 1111–1123 (1989).
47. M. Oldani and A. Bauer, *Chem. Phys. Lett.* **108**, 7–10 (1984).
48. S. Doraiswamy and S. D. Sharma, *J. Mol. Struct.* **102**, 81–92 (1983).
49. E. Fliege, H. Dreizler, S. Gerber, and H. Huber, *J. Mol. Spectrosc.* **137**, 24–32 (1989).
50. P. N. Ghosh, C. E. Blom, and A. Bauder, *J. Mol. Spectrosc.* **89**, 159–173 (1981).
51. R. L. DeLeon and J. S. Muentner, *J. Chem. Phys.* **72**, 6020–6023 (1980); *J. Mol. Spectrosc.* **126**, 13–18 (1987).
52. M. D. Marshall and W. A. Klemperer, *J. Chem. Phys.* **81**, 2928–2932 (1984).
53. O. Böttcher, N. Heineking, M. Andolfatto, and D. H. Sutter, *Z. Naturforsch.* **44a**, 89–94 (1989).
54. A. Baldacci, S. Gherseti, S. C. Hurlock, and K. N. Rao, *J. Mol. Spectrosc.* **59**, 116–125 (1976).
55. W. H. Stolze and D. H. Sutter, *Z. Naturforsch.* **39a**, 1092–1103 (1984).
56. E. Fliege, H. Dreizler, and B. Kleimömer, *J. Mol. Struct.* **97**, 225–228 (1983).
57. L. M. Tach and S. G. Kukolich, *J. Chem. Phys.* **78**, 6512–6514 (1983).
58. V. W. Weiss and W. H. Flygare, *J. Chem. Phys.* **45**, 8–10 (1966).
59. P. Botschwina, M. Horn, S. Seeger, and J. Fluegge, *Mol. Phys.* **78**, 191–198 (1993).
60. G. Strey and I. M. Mills, *Mol. Phys.* **26**, 129–138 (1973).
61. S. L. Hartford, W. C. Allen, C. L. Norris, E. F. Perarson, and W. H. Flygare, *Chem. Phys. Lett.* **18**, 153–157 (1973).
62. U. P. Verma, K. Möller, J. Vogt, M. Winnewisser, and J. J. Christiansen, *Can. J. Phys.* **63**, 1173–1183 (1985).
63. E. F. Pearson and W. Gordy, *Phys. Rev.* **177**, 59–61 (1969).
64. E. Rothstein, *J. Chem. Phys.* **50**, 1899–1900 (1969).